GENERALIZED BIPYRAMIDS AND HYPERBOLIC VOLUMES OF TILING LINKS

COLIN ADAMS, AARON CALDERON, XINYI JIANG, ALEXANDER KASTNER, GREGORY KEHNE, NATHANIEL MAYER, AND MIA SMITH

Abstract. We present explicit geometric decompositions of the complement of *tiling links*, which are alternating links whose projection graphs are uniform tilings of S^2, $\mathbb{E}^2$, or $\mathbb{H}^2$. This requires generalizing the angle structures program of Casson and Rivin for triangulations with a mixture of finite, ideal, and truncated (i.e. ultra-ideal) vertices. A consequence of this decomposition is that the volumes of spherical tiling links are precisely twice the maximal volumes of the ideal Archimedean solids of the same combinatorial description. In the case of hyperbolic tiling links, we are led to consider links embedded in thickened surfaces $S_g \times I$ with genus $g \geq 2$. We generalize the bipyramid construction of Adams to truncated bipyramids and use them to prove that the set of possible volume densities for links in $S_g \times I$, ranging over all $g \geq 2$, is a dense subset of the interval $[0, 2v_{\text{oct}}]$, where $v_{\text{oct}} \approx 3.66386$ is the volume of the regular ideal octahedron.

1. Introduction

For many links L embedded in 3-manifolds M, the complement $M - L$ admits a unique hyperbolic structure. In such cases we say that the link is hyperbolic, and denote the hyperbolic volume of the complement by $\text{vol}(L)$, leaving the identity of M implicit. Computer programs like Jeff Weeks' SnapPea allow for easy numerical computation of these volumes, but simple theoretical computations are rare. In [CKP15a], Champanerkar, Kofman, and Purcell present an explicit geometric decomposition of the complement of the infinite square weave, the infinite alternating link whose projection graph is the square lattice $\mathcal{W}$ (see Figure 1), into regular ideal octahedra, one for each square face of the projection. The volume of the infinite link complement is infinite, but it is natural to study instead the *volume density*, defined as $\mathcal{D}(L) = \text{vol}(L)/c(L)$ where $c(L)$ is the crossing number. For infinite links with symmetry like $\mathcal{W}$, we can make this well defined by taking the volume density of a single fundamental domain. Since faces of $\mathcal{W}$ are in bijective correspondence with crossings, the decomposition of [CKP15a] shows the volume density to be $\mathcal{D}(\mathcal{W}) = v_{\text{oct}} \approx 3.66386$, the volume of the regular ideal octahedron.

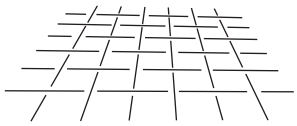

Figure 1. The infinite square weave link $\mathcal{W}$, a tiling link derived from the 4.4.4.4 tiling of the Euclidean plane.

In this paper we generalize their example and give explicit geometric decompositions and volume density computations for all *tiling links*, alternating links whose projection graphs are uniform tilings of the sphere (embedded in S^3), the Euclidean plane (in $\mathbb{R}^3$), or the hyperbolic plane (in $\mathbb{R}^2 \times I$). In the latter two cases, we avoid working directly with infinite links by taking a quotient of the infinite link complement by a discrete subgroup of the symmetry group, yielding a finite link complement in a thickened torus $T \times (0, 1)$ for Euclidean tilings and thickened higher genus surfaces for hyperbolic tilings, denoted $S_g \times I$ where g is the genus. These surfaces are permitted to be non-orientable, in which case the genus is defined as $g = (2 - \chi)/2$ where χ is the Euler characteristic. This definition differs from the standard "non-orientable genus" by a factor of 2, with the benefit that all surfaces of a given genus have equal Euler characteristic, though in exchange surfaces may have half-integer genus. When the specific genus is unimportant, we use $S \times I$ to denote any thickened surface of genus $g \geq 2$. The crossing number of a link in $S \times I$ is defined as the minimal

Date: March 14, 2016.

number of crossings across all possible projections onto $S \times \{0\}$. It was proven in [AFLT02] that $c(L)$ is realized for a reduced alternating projection of L onto $S \times \{0\}$.

The analysis of hyperbolic tiling links yields independent results about link complements in $S \times I$. We show that volume densities for links in $S \times I$ are bounded above by $2v_{\text{oct}}$. For links in $S_g \times I$ with fixed genus $g \geq 2$, the volume density is bounded by a number $\beta_g < 2v_{\text{oct}}$, related to the volume of generalized hyperbolic n-bipyramids with all dihedral angles $\pi/2$. These bipyramid volumes are bounded by and asymptotically approach $v_{\text{oct}}n/2$, and the bounds β_g correspondingly approach $2v_{\text{oct}}$ for large g. We show that tiling links derived from the 4-regular hyperbolic $(8g-4)$-gon tilings achieve the maximal volume density β_g for each g, and use these to prove the set of all possible volume densities in $S \times I$ is dense in the interval $[0, 2v_{\text{oct}}]$. As a corollary to the proof, we have that volume densities for links in the thickened torus $T \times (0,1)$, known to be bounded above by v_{oct}, are in fact dense in the interval $[0, v_{\text{oct}}]$. This extends previous results that volume densities are dense in $[0, v_{\text{oct}}]$ for knots in S^3 [Bur15], [ACJ+15].

Our decomposition is based on work in [Ada15a], which in turn is based on a construction due to D. Thurston, breaking up the complement of a link in S^3 into octahedra using one at each crossing. These octahedra have two ideal vertices, located on the cusps at that crossing, and four finite vertices which are identified in pairs to two finite points. The two points are thought of as being far above and below the projection sphere for the link, and we denote them U and D. Any such octahedron has volume less than v_{oct}, so this gives an upper bound on the volume of the link, $\text{vol}(L) \leq v_{\text{oct}}c(L)$. The bound can be improved slightly by collapsing edges or drilling, though asymptotically there exist links whose volume densities approach v_{oct} [CKP15a].

In [Ada15a], the octahedral decomposition is rearranged into face-centered bipyramids. Thurston's octahedra are cut open along the core vertical line connecting the ideal vertices, yielding four tetrahedra. The tetrahedra each have two ideal and two finite vertices, identified with U and D. The edge connecting the finite vertices passes through the center of one of the four faces adjacent to the crossing for that octahedron, as shown in Figure 2. This edge is shared by one tetrahedron from each crossing bordering that face, which glue together to form a bipyramid. The apexes of the bipyramids are the finite vertices U and D, while the vertices around the central polygon are ideal. Any such n-bipyramid has volume less than the maximal volume ideal n-bipyramid, shown in [Ada15a] to be regular, with volume bounded above by and asymptotically approaching $2\pi \log(n/2)$. These bipyramids are denoted B_n^{ideal}. The construction puts an upper bound on volume

$$\text{vol}(L) < \sum_i \text{vol}(B_{n_i}^{\text{ideal}})$$

where n_i denotes the number of edges in the i-th face of the projection of L, and drilling or collapsing allows the removal of the two largest bipyramids from the sum. For link projections whose faces have many edges, this gives a dramatically better bound than Thurston's octahedra.

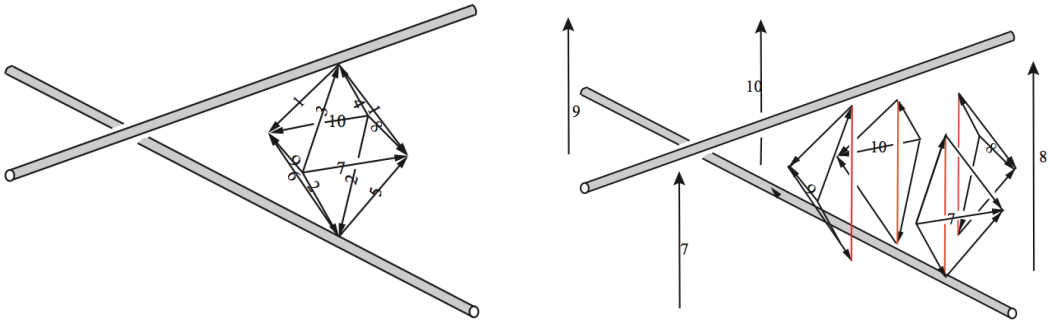

FIGURE 2. Cutting up octahedra to reassemble into face-centered bipyramids.

Much of this paper is devoted to generalizing the bipyramid decomposition for links in $T \times (0,1)$ and $S \times I$, and then exploiting the symmetry of tiling links to precisely determine the dihedral angles in the complete hyperbolic structure. In Section 2, we present relevant background on generalized hyperbolic polyhedra and extend the angle structures program of Casson and Rivin to allow for a mixture of finite, ideal, and truncated (i.e. ultra-ideal) vertices. Section 3 deals with the maximal volumes for certain classes

of generalized polyhedra which appear in the generalized octahedral and bipyramidal decompositions. These results are then applied in Section 4 to tiling links, allowing us to calculate exact volume densities for all links associated to 3- or 4-regular uniform tilings. Section 4 also contains results on the set of volume densities for links in thickened surfaces.

2. Generalized angle structures

A *generalized hyperbolic tetrahedron* is the convex hull of four points which may be *finite* (within $\mathbb{H}^3$), *ideal* (on $\partial\mathbb{H}^3$), or *ultra-ideal* (outside $\mathbb{H}^3 \cup \partial\mathbb{H}^3$). Ultra-ideal points fit most naturally into the Klein ball model of $\mathbb{H}^3$. Given an ultra-ideal point x outside the unit sphere in $\mathbb{R}^3$, consider the cone of lines through x tangent to the sphere. The canonical truncation plane associated to x is the plane containing the circle where that cone intersects the sphere. Geodesic lines and planes through the ultra-ideal point are computed as Euclidean lines and planes through the point as usual, cut off at the truncation plane (see Figure 3). Note that all edges of the tetrahedron that passed through x before truncation are prependicular to the corresponding truncation plane. For more background on ultra-ideal points, see, *e.g.*, [Ush06].

We will often prefer to work in the Poincaré ball model for computing lengths and angles. Since the two models agree on the sphere at infinity, we can do this by using the Klein model to locate the ideal boundaries of geodesic lines and planes, and then construct the geodesics corresponding to those boundaries in the Poincaré model.

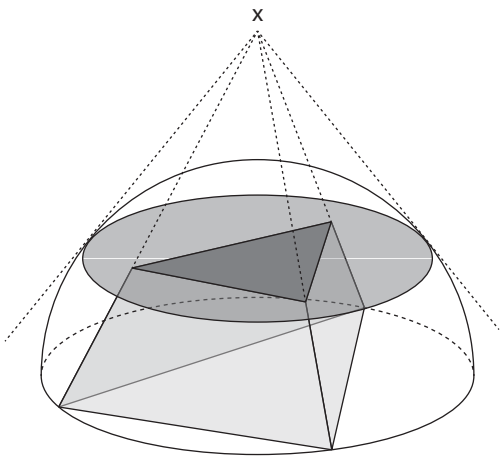

Figure 3. The canonical truncation of an ultra-ideal point in the Klein ball model.

A generalized hyperbolic tetrahedron is fully determined by its six dihedral angles. We can thus specify a tetrahedron with a vector $\Delta = (A, B, C, D, E, F) \in [0, \pi]^6$, with the dihedral angles labelled as in Figure 4. We restrict our attention to *mildly truncated* tetrahedra, those in which truncation planes for distinct ultra-ideal vertices do not intersect within $\mathbb{H}^3$. It should be understood that all truncated tetrahedra in this paper are mildly truncated. In this case there is a formula for the volume of a generalized tetrahedron in terms of its dihedral angles.

Theorem 2.1 ([Ush06])**.** *Given a generalized hyperbolic tetrahedron Δ with dihedral angles as in Figure 4, let*

$$a = e^{iA},\ b = e^{iB},\ ...,\ f = e^{iF},$$

$$G = \begin{pmatrix} 1 & -\cos A & -\cos B & -\cos F \\ -\cos A & 1 & -\cos C & -\cos E \\ -\cos B & -\cos C & 1 & -\cos D \\ -\cos F & -\cos E & -\cos D & 1 \end{pmatrix},$$

$$z_1 = -2\frac{\sin A \sin D + \sin B \sin E + \sin C \sin F - \sqrt{\det G}}{ad + be + cf + abf + ace + bcd + def + abcdef},$$

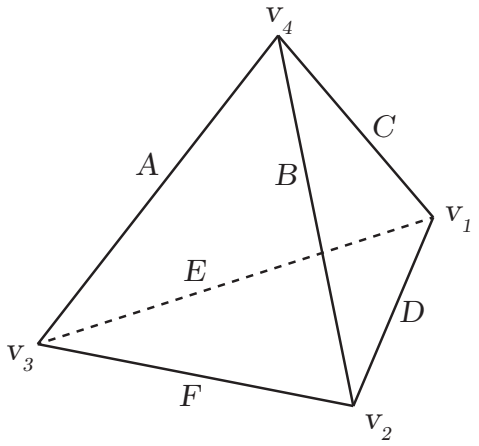

FIGURE 4. A tetrahedron with vertices and dihedral angles labeled.

$$z_2 = -2\frac{\sin A \sin D + \sin B \sin E + \sin C \sin F + \sqrt{\det G}}{ad + be + cf + abf + ace + bcd + def + abcdef},$$

$$U(z,\Delta) = \frac{1}{2}(Li_2(z)+Li_2(abdez)+Li_2(acdfz)+Li_2(bcefz)-Li_2(-abcz)-Li_2(-aefz)-Li_2(-bdfz)-Li_2(-cdez)),$$

where $Li_2(z)$ is the dilogarithm function, defined by the analytic continuation of the integral

$$Li_2(x) = -\int_0^x \frac{\log(1-t)}{t}\,dt$$

for $x \in \mathbb{R}_{>0}$. Then the volume of Δ is given by

$$\mathrm{vol}(\Delta) = \frac{1}{2}Im(U(z_1,\Delta) - U(z_2,\Delta)).$$

The generalized volume formula in terms of the angles is unwieldy, but the total differential takes an elegant form in terms of the edge lengths. This is Schläfli's differential formula, in the three-dimensional case (see, *e.g.* [Sch50], [Kel89]).

Theorem 2.2 (Schläfli's differential formula)**.** *Given a generalized hyperbolic tetrahedron Δ with dihedral angles θ_i and corresponding edge lengths ℓ_i, the differential of the volume function is given by*

$$d\mathrm{vol}(\Delta) = -\frac{1}{2}\sum_{i=0}^{6} \ell_i\, d\theta_i.$$

Let M be a compact hyperbolic 3-manifold, either without boundary or with totally geodesic boundary, and let T be a triangulation of M by a collection of tetrahedra which may have finite, ideal, or ultra-ideal vertices. An *angle structure* on T is an assignment of dihedral angles in the range $[0,\pi]$ to each edge in each tetrahedron, such that

(i) the sum of the dihedral angles around any one edge equals 2π, and
(ii) the sum of the three dihedral angles incident to an ideal vertex in a single tetrahedron equals π.
(iii) the sum of the dihedral angles around an ultra-ideal vertex is less than π.
(iv) the sum of the dihedral angles incident to a finite vertex is greater than π.

An angle structure on a triangulation consisting of n tetrahedra is thus given by a vector $\Theta \in \mathcal{A} \subset [0,\pi]^{6n}$, where $\mathcal{A}$ is a bounded open set defined by the above constraints. The total volume of the tetrahedra in an angle structure is denoted $\mathrm{vol}(\Theta)$. Casson and Rivin's original program deals exclusively with ideal triangulations, but their key results hold in this more general context.

Theorem 2.3. *Let $\mathcal{A}$ be the space of angle structures for a triangulation of a compact hyperbolic 3-manifold M, boundaryless or with totally geodesic boundary. Then a critical point of the volume functional on $\mathcal{A}$ gives a complete hyperbolic structure for M.*

Proof. The case where all vertices are ideal is Rivin's original result, proofs of which can be found in [Riv94] and [FG11].

Triangulations with a mixture of ideal and ultra-ideal vertices are discussed in [LST08], [LY14] and by Frigerio and Petronio in [FP04]. Most of the discussion there applies equally well to triangulations with finite vertices. They show that an angle structure gives a complete hyperbolic structure (with totally geodesic boundary if applicable) if and only if it satisfies four conditions:

(i) The sum of the dihedral angles around a single edge is 2π.
(ii) Identified faces are isometric.
(iii) There are no shearing singularities around edges with two ideal endpoints.
(iv) A completeness condition is satisfied at each cusp.

Condition (i) is part of the definition of an angle structure, so it is satisfied automatically.

In most cases, Condition (ii) is satisfied if identified vertices are of the same type and all finite lengths of identified edges in identified faces are equal. This is true at any critical point of the volume functional. Suppose e and e' are identified edges with finite lengths (i.e. no ideal endpoints), with corresponding dihedral angles θ and θ'. Then there is a deformation vector in the tangent space of $\mathcal{A}$ which increments θ and decrements θ'. At a critical point of the volume functional on $\mathcal{A}$, we have

$$\frac{\partial \mathrm{vol}(\Theta)}{\partial \theta} = \frac{\partial \mathrm{vol}(\Theta)}{\partial \theta'},$$

and substitution by the Schläfli formula gives

$$\ell_e = \ell_{e'}.$$

Thus glued edges between finite vertices must have the same edge lengths. However, we must still account for those finite lengths that are generated by truncation, i.e. which lie along the truncation plane. In these cases, the Schläfli formula and hyperbolic geometry imply that the finite truncation edges have equal lengths. We discuss one such case and leave the rest to the enterprising reader. In cases which involve ideal vertices, the argument must be modified by considering the distance between concentric horocycles as described below for exceptional hexagons.

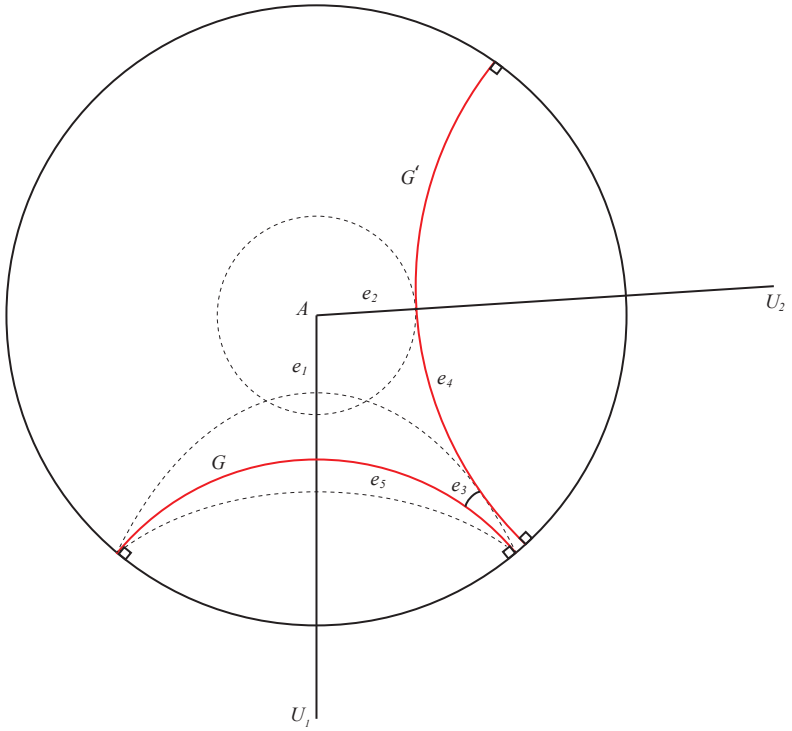

FIGURE 5. The lengths ℓ_1, ℓ_2 and ℓ_3 together with vertex types determine ℓ_4 and ℓ_5.

Consider a face with one finite vertex A and two ultra-ideal vertices U_1 and U_2 as in Figure 5. We let ℓ_1 denote the length of e_1 and so on. By isometries we may assume that the finite vertex A is at the origin, and that one of the ultra-ideal vertices U_1 lies on the y-axis below it. The Schläfli formula then gives that

$$\begin{aligned} \ell_1 &= \ell_1' \\ \ell_2 &= \ell_2' \\ \ell_3 &= \ell_3'. \end{aligned}$$

Define a geodesic hyperplane G perpendicular to the edge from A to U_1 such that the distance from G to A is ℓ_1. Consider the inside ℓ_3 banana neighborhood of G and the ℓ_2 neighborhood of A. As A was taken to be the origin, the (Euclidean) radius of a geodesic hyperplane tangent to the ℓ_2 sphere around F is constant, while along the banana neighborhood the radius of curvature of the tangent geodesic increases continuously as the point of tangency moves inwards and decreases again once it moves out. Thus there exists at most one (up to reflection) geodesic hyperplane G' tangent to both neighborhoods and the lengths ℓ_4 and ℓ_5 are determined by ℓ_1, ℓ_2 and ℓ_3. Hence

$$\begin{aligned} \ell_4 &= \ell_4' \\ \ell_5 &= \ell_5' \end{aligned}$$

and faces must then be isometric.

Vertex types and finite edge lengths are not enough to determine the isometry type of two of these classes of generalized triangles. The first are the so called "exceptional hexagons" from [FP04], generalized triangles with one ideal and two ultra-ideal vertices such that the two truncation arcs are tangent, so the length of the internal edge between them is 0. Given such a face F on a tetrahedron Δ, we call the two edges of F incident to the ideal vertex e_1 and e_2, and the dihedral angles of Δ along those edges θ_1 and θ_2 respectively.

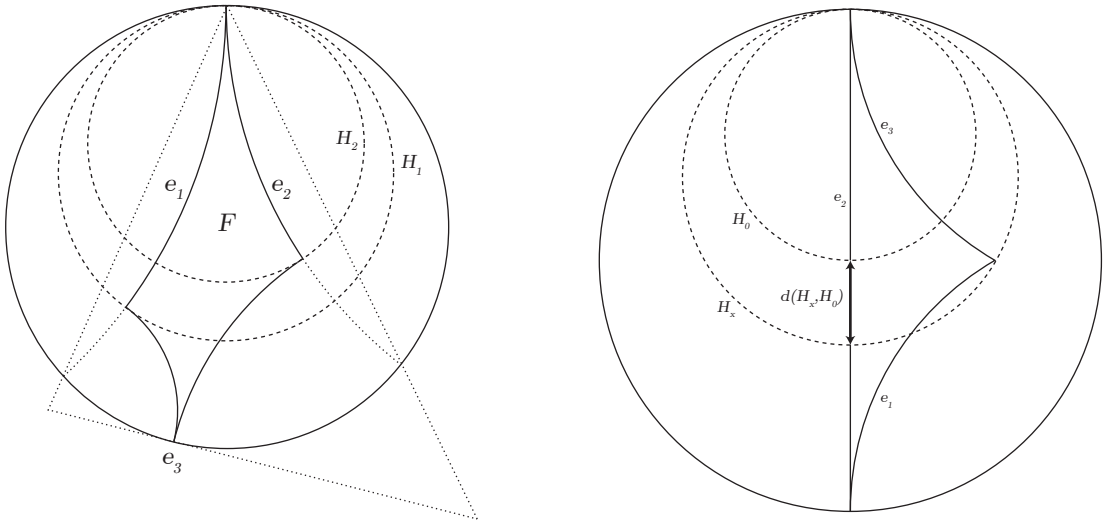

(A) An "exceptional hexagon." (B) A triangle with one finite and two ideal vertices.

FIGURE 6. Triangles whose isometry types are not fully determined by their vertex types and edge lengths.

The notion of a circle around an ideal point is captured by horocircles, which in the Poincaré disk model are Euclidean circles tangent to $\partial\mathbb{H}^2$ at their ideal "center". The hyperbolic radius of a horocircle is always infinite, so throughout this paper the radius of a horocircle should be understood as its Euclidean radius in the Poincaré disk model. Two horocircles centered at the same ideal point behave appropriately as concentric circles, which is to say that the shortest path between them is achieved by following any geodesic ending at the ideal center. Horospheres in higher dimensions are analogous.

We consider concentric horocircles H_1 and H_2, centered at the ideal vertex of F, passing through the opposite ends of e_1 and e_2 respectively, as shown in Figure 6a. The finite distance between H_1 and H_2 determines F up to isometry. If such a face F is identified to a corresponding face F' on a tetrahedron Δ',

then there is a deformation vector in the tangent space of $\mathcal{A}$ which increments θ_1 and θ_2' and decrements θ_2 and θ_1'. This maintains the appropriate sum of dihedral angles incident on the ideal vertex, as well as the sum of the angles around each edge. Using Schläfli's formula again, the angle structure at a critical point of the volume functional must satisfy

$$\ell_1 - \ell_2 = d(H_1, H_2) = \ell_1' - \ell_2' = d(H_1', H_2'),$$

thus F and F' are isometric.

The second type of problematic triangle is that with one finite vertex and two ideal vertices. As with the exceptional hexagons, these are problematic because all edge lengths are infinite. In the Poincaré disk model, we may assume the vertices of such a triangle are $(0, \pm 1)$ and $(x, 0)$. Label the three edges e_1, e_2, e_3 as shown in Figure 6b, with corresponding dihedral angles $\theta_1, \theta_2, \theta_3$. Consider concentric horocircles H_x and H_0, centered at $(0, 1)$, passing through $(x, 0)$ and the origin respectively. The triangle is determined up to isometry by $d(H_x, H_0)$. Suppose that two such exceptional triangles F and F' are identified. Then there exists a vector in the tangent space of $\mathcal{A}$ which increments θ_1, θ_3, and θ_2', and decrements $\theta_2, \theta_1', \theta_3'$. At a critical point of the volume functional, by Schläfli's formula and the symmetry of the triangles we have

$$\ell_1 + \ell_3 - \ell_2 = 2d(H_x, H_0) = \ell_1' + \ell_3' - \ell_2' = 2d(H_x', H_0'),$$

so F and F' are again isometric.

Conditions (iii) and (iv) deal only with the ideal vertices. Every ideal vertex in a tetrahedron can be assigned a complex shape parameter, independent of the other vertices. Those shape parameters can be used to compute holonomy exactly as in the entirely ideal case. As shown in [FG11], conditions (iii) and (iv) can be written solely in terms of holonomy, and they are satisfied at a critical point of the volume functional. □

Triangulations with ultra-ideal vertices occur when considering manifolds with totally geodesic boundaries. Under the assumption of total geodesicity of the boundary, doubling and the Mostow rigidity theorem imply the following.

Theorem 2.4. *On any manifold M there exists at most one finite-volume complete hyperbolic structure with totally geodesic boundary.*

3. Maximal generalized tetrahedra and bipyramids

Both Thurston's octahedral construction and the bipyramid construction decompose into generalized tetrahedra with two ideal vertices.

Lemma 3.1. *Let Δ be a tetrahedron labelled as in Figure 4 with v_1 and v_2 ideal vertices. For fixed angle $A \in [0, \pi]$, the maximal volume for such a tetrahedron is achieved when the other angles are*

$$D = \arccos\left(\frac{1}{2}(\cos A - 1)\right),$$

$$B = C = E = F = \frac{\pi - D}{2}.$$

In this case v_3 and v_4 are ultra-ideal.

Proof. The condition that v_1 and v_2 are ideal vertices imposes the constraints

$$B + F + D = C + E + D = \pi.$$

We use Lagrange multipliers to maximize the volume subject to those constraints.

$$\frac{\partial \mathrm{vol}}{\partial B} = \frac{\partial \mathrm{vol}}{\partial F} = \lambda$$

$$\frac{\partial \mathrm{vol}}{\partial C} = \frac{\partial \mathrm{vol}}{\partial E} = \mu$$

$$\frac{\partial \mathrm{vol}}{\partial D} = \lambda + \mu$$

By Schläfli's differential formula, those equations become

$$\ell_B = \ell_F$$
$$\ell_C = \ell_E$$
$$\ell_D = \ell_B + \ell_C.$$

However, all these edges have at least one ideal endpoint, so the lengths are infinite. To recover useful information from Schläfli's formula, we replace the ideal vertices with finite vertices $\bar{v}_1$ and $\bar{v}_2$ and consider the limiting behavior as they approach the ideal points v_1 and v_2. That is, we require

$$\lim_{\bar{v}_2 \to v_2} (\ell_B - \ell_F) = \lim_{\bar{v}_1 \to v_1} (\ell_C - \ell_E) = \lim_{\substack{\bar{v}_1 \to v_1 \\ \bar{v}_2 \to v_2}} (\ell_D - \ell_B - \ell_C) = 0.$$

Up to isometries of $\mathbb{H}^3$ in the Poincaré ball model, we may let $v_1 = (0, 0, -1)$, $v_2 = (0, 0, 1)$, and $v_4 = (r_4, 0, 0)$, as in Figure 7. Then v_3 lies at some point

$$v_3 = (r_3 \cos D \sin \phi, r_3 \sin D \sin \phi, r_3 \cos \phi).$$

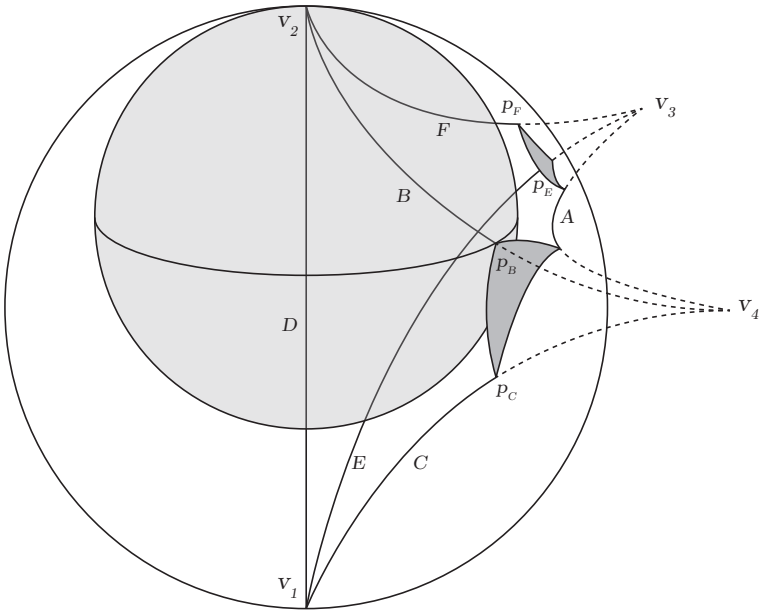

FIGURE 7. A truncated tetrahedron as in Lemma 3.1.

Let p_B, p_C, p_E, p_F be the endpoints of edges B, C, E, and F respectively, opposite from v_1 and v_2. That is, if v_4 is finite or ideal then $p_B = p_C = v_4$, but if v_4 is ultra-ideal then p_B and p_C are the intersections of their respective edges with the truncation plane for v_4, and similarly for p_E and p_F. The point p_B lies on a unique horosphere centered at v_2, given by

$$x^2 + y^2 + (z - (1 - R_B))^2 = R_B^2$$

for some $R_B \in [0, 1]$. By symmetry, p_C lies on an opposite horosphere of the same radius centered at v_1. Similarly p_E and p_F lie on horospheres of radii R_E, R_F around v_1 and v_2 respectively. As $\bar{v}_1$ and $\bar{v}_2$ become ideal, $\ell_B - \ell_F$ limits to the finite distance between the concentric horospheres of radii R_B and R_F, and similarly $\ell_C - \ell_E$ limits to the distance between concentric horospheres of radii R_B and R_E. Furthermore, since we can split edge D at the origin, $\ell_D - \ell_B - \ell_C$ tends to twice the distance between concentric horospheres of radii R_B and $\frac{1}{2}$. Thus the optimization conditions become

$$R_E = R_F = R_B = \frac{1}{2}.$$

This is satisfied if v_3 and v_4 lie at the origin, but then Δ is degenerate, with volume 0. Alternatively the truncation planes for v_3 and v_4 must both be mutually tangent to the two horospheres of radius $\frac{1}{2}$ centered at v_1 and v_2. Therefore v_3 must be equidistant from the Euclidean centers of the horospheres $(0, 0, \pm\frac{1}{2})$, so it must lie on the xy-plane. Thus $\phi = \pi/2$. At this point we can see by symmetry of the tetrahedron and the ideal vertex constraints that

$$B = C = E = F = \frac{\pi - D}{2}.$$

The Euclidean radius of the truncation plane for v_3 is $\sqrt{r_3^2 - 1}$, so we have by the Pythagorean theorem

$$\left(\sqrt{r_3^2 - 1} + \frac{1}{2}\right)^2 = r_3^2 + \left(\frac{1}{2}\right)^2$$

which implies $r_3 = \sqrt{2}$. By the same reasoning $r_4 = \sqrt{2}$. Thus $v_4 = (\sqrt{2}, 0, 0)$ and $v_3 = (\sqrt{2}\cos D, \sqrt{2}\sin D, 0)$.

Finally we compute an explicit relationship between A and D. The top and bottom faces of this tetrahedron are given by

$$\left(x - \frac{1}{\sqrt{2}}\right)^2 + \left(y - \frac{1 - \cos D}{\sqrt{2}\sin D}\right)^2 + (z \pm 1)^2 = \frac{1 - \cos D}{\sin^2 D},$$

and the angle between them is

$$A = \arccos(1 + 2\cos D).$$

Inverting the function, we arrive at

$$D = \arccos\left(\frac{1}{2}(\cos A - 1)\right).$$

□

Corollary 3.2. *The maximal volume generalized tetrahedron with two ideal vertices has volume $v_{oct}/2$, with angles*

$$A = 0, \quad D = \frac{\pi}{2}, \quad B = C = E = F = \frac{\pi}{4}.$$

Proof. We see immediately from the Schläfli formula that decreasing any one angle increases the volume. Thus among tetrahedra with two ideal vertices as described in Lemma 3.1, the maximal volume occurs when $A = 0$. The other angles follow from the formulas in the lemma. The volume of this tetrahedron is $v_{\text{oct}}/2$. □

In Thurston's octahedral construction, these tetrahedra assemble into octahedra with two opposite ideal vertices.

Corollary 3.3. *The maximal volume of a generalized hyperbolic octahedron with two opposite ideal vertices is $2v_{oct}$.*

Proof. A generalized hyperbolic octahedron with two opposite ideal vertices can be cut into four tetrahedral wedges around the core line connecting the ideal vertices. All four of these wedges may be the maximal tetrahedron described in Corollary 3.2, with the dihedral angles gluing together along the core line all equal to $\pi/2$. The volume is then $4(v_{\text{oct}}/2) = 2v_{\text{oct}}$. This generalized octahedron is shown in Figure 8. □

Lemma 3.1 also allows us to determine the maximal bipyramids with ideal vertices around the central polygon and ultra-ideal apexes.

Corollary 3.4. *The maximal volume generalized n-bipyramid with ideal vertices around the central polygon is made of n identical maximal volume tetrahedra of the type described in Lemma 3.1, with angles $A = 2\pi/n$.*

Proof. A generalized n-bipyramid with ideal vertices around the central polygon can be cut along its core line into tetrahedra $\Delta_1, ..., \Delta_n$, each with two ideal vertices. Label the edges of each as in Figure 7, with subscripts to distinguish the tetrahedron to which they belong. The ideal vertices on each tetrahedron dictate the constraints

$$B_i + F_i + D_i = C_i + E_i + D_i = \pi,$$

and the fact that the tetrahedra are all glued together along the core line additionally requires

$$\sum_{i=1}^{n} A_i = 2\pi.$$

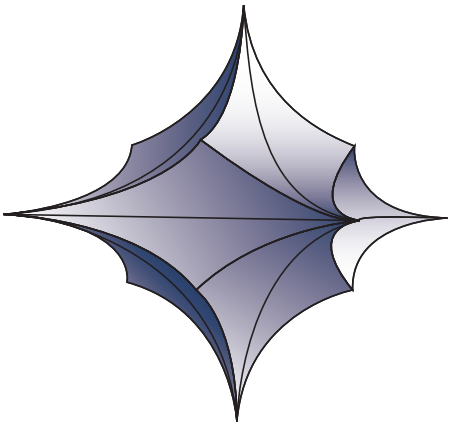

FIGURE 8. The maximal volume generalized hyperbolic octahedron with two opposite ideal vertices. The other four vertices are ultra ideal, with length 0 edges between them collapsing into ideal vertices.

We maximize using Lagrange multipliers and substitute from Schläfli's formula, obtaining the equations

$$\begin{aligned}\ell_{A_i} &= \ell_{A_j}\\ \ell_{B_i} &= \ell_{F_i}\\ \ell_{C_i} &= \ell_{E_i}\\ \ell_{D_i} &= \ell_{B_i} + \ell_{C_i}\end{aligned}$$

for all i, j. By the same logic used in the proof of Lemma 3.1, the last three equations imply that Δ_i is isometric to a tetrahedron in the Poincaré ball model with vertices

$$v_1^i = (0,0,-1), \quad v_2^i = (0,0,1), \quad v_4^i = (\sqrt{2},0,0), \quad v_3^i = (\sqrt{2}\cos D_i, \sqrt{2}\sin D_i, 0).$$

In this model it is apparent that ℓ_{A_i} increases monotonically with D_i. Thus $\ell_{A_i} = \ell_{A_j}$ implies $D_i = D_j$, and consequently $A_i = A_j = 2\pi/n$. The other angles depend on A_i as in the lemma because the tetrahedra are maximal. □

We refer to the bipyramids described in 3.4 as *maximal doubly truncated n-bipyramids*, denoted $B_n^{\text{truncated}}$. Some volumes of these bipyramids are shown in Figure 9b. We note that the ratio

$$\frac{\text{vol}(B_n^{\text{truncated}})}{n}$$

is strictly increasing with n, asymptotically approaching $v_{\text{oct}}/2$ as the tetrahedral wedges making up the bipyramids approach the maximal wedge (with angle $A = 0$) discussed in Corollary 3.2. This contrasts with the case of ideal bipyramids, where

$$\lim_{n\to\infty} \frac{\text{vol}(B_n^{\text{ideal}})}{n} = 0,$$

peaking when $n = 6$ at v_{tet}, the volume of a regular ideal tetrahedron.

4. Tiling Links

Given a 4-regular uniform tiling of the Euclidean plane, we may define an associated *tiling link* $\widetilde{L}$ to be an alternating link derived by assigning an oriented crossing to each vertex (see Figure 10a). This definition can be generalized to 3-regular uniform tilings by choosing one of the three edges at each vertex to "double", which corresponds to adding bigons in the associated tiling link. This is always possible by applying Petersen's theorem to a fundamental domain (see, *e.g.* [Pet91], [Bra17]), which further ensures that the link with bigons is invariant under some two linearly independent translations. Note that this process can result in multiple associated tiling links, defined both by how we choose chirality and where we choose

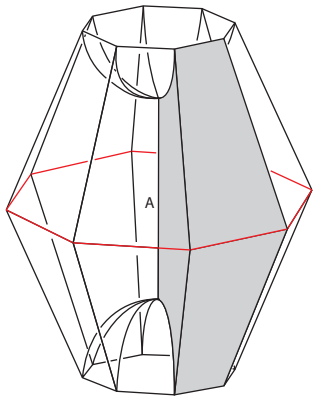

(A) A doubly truncated 8-bipyramid with angle $A = \frac{\pi}{4}$.

n	$\mathrm{vol}(B_n^{\mathrm{truncated}})$
2	0
3	2.6667
4	5.0747
5	7.3015
6	9.4158
7	11.4580
8	13.4520
9	15.4122
10	17.3481
100	183.0944
1000	1831.9213

(B) Volumes of maximal doubly truncated n-bipyramids.

FIGURE 9. Maximal doubly truncated bipyramids.

to add bigons. For example, the 3.6.3.6 tiling is chiral and the 6.6.6 tiling has an infinite number of ways we may add bigons to make it a 4-regular graph. Our results hold independently of the choice of bigons.

Just as with Euclidean tilings, we define a tiling link associated to a uniform hyperbolic tiling to be an infinite alternating link $\widetilde{L}$ derived from a hyperbolic tiling by changing vertices into crossings and adding bigons where necessary. See Figure 10b for an example. Again bigons may be added such that the link has compact fundamental domain. We may use a similar process to obtain links derived from spherical tilings, which correspond precisely to Archimedean polyhedra.

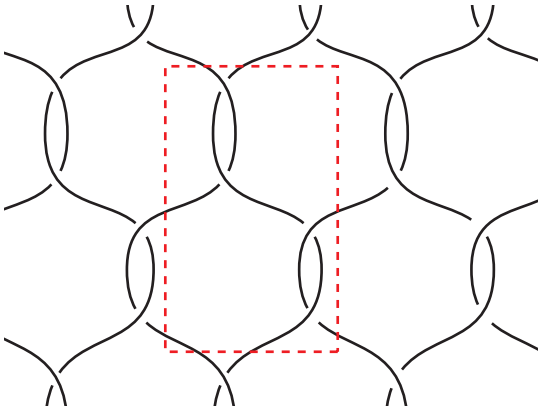

(A) A tiling link derived from the 6.6.6 tiling of $\mathbb{E}^2$

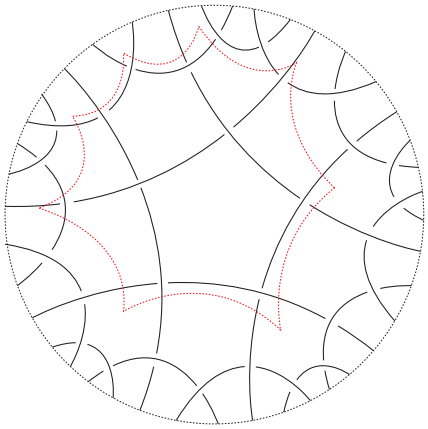

(B) A tiling link derived from the 5.5.5.5 tiling of $\mathbb{H}^2$

FIGURE 10. Tiling links shown with fundamental domains for appropriate surface groups.

4.1. **Tiling links in thickened surfaces.** To determine the appropriate ambient space in which to embed the infinite tiling links, we look for an appropriate generalization of the bipyramid decomposition of [Ada15a] for these infinite objects. After carrying out the bipyramid decomposition on a typical link $L \subset S^3$, consider a small sphere S centered around the finite point U. That sphere intersects each n-bipyramid in an n-gon, which we call the *vertex link* of U in that bipyramid. All together, the vertex links of U across all the bipyramids tile the sphere S, and that tiling is an exact copy of the projection graph of L. The same behavior occurs around the other apex D.

In an analogous bipyramid construction for a Euclidean tiling link, the vertex links of a shared apex across all the bipyramids should form a copy of the Euclidean projection graph, which is to say the original tiling. However, the vertex link of a finite vertex in any convex hyperbolic polyhedron is a spherical polygon. For the vertex links to be Euclidean polygons, the apex must be an ideal point. That is, it must lie on a cusp, and

since the vertex links form an infinite Euclidean tiling, it must be an infinite planar cusp, the boundary of a neighborhood of infinity. Thus Euclidean tiling links are most naturally embedded in $\mathbb{R}^3$. We may think of the transition between the standard bipyramid decomposition and this Euclidean bipyramid decomposition as pushing the finite points U and D out towards infinity as more faces are added to the link projection. To corroborate this notion, Champanerkar, Kofman, and Purcell prove in [CKP15b] that the complements $S^3 - W(p,q)$ approach $\mathbb{R}^3 - \mathcal{W}$ as a geometric limit, where the weaving links $W(p,q)$ are increasing finite patches of the infinite square weave $\mathcal{W}$.

Similarly, for hyperbolic tiling links, the vertex links of a shared apex in the bipyramids should be hyperbolic polygons, which forces the apex to be ultra-ideal. The bipyramids are then truncated, so the vertex links form a hyperbolic tiling of the totally geodesic truncation plane. Thus hyperbolic tiling links are most naturally embedded in $\mathbb{R}^2 \times I$. It should be noted that Thurston's octahedral construction generalizes along with the bipyramid decomposition, simply by sending U and D to be ideal or ultra-ideal rather than finite. Figure 11 depicts the octahedral decomposition in the ultra-ideal case.

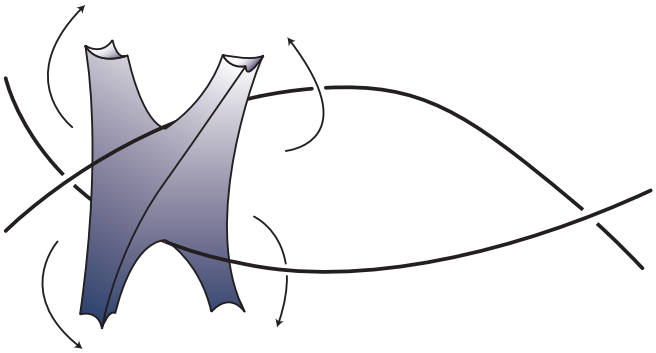

FIGURE 11. The decomposition of $(\mathbb{R}^2 \times I) - L$ by truncated octahedra.

Instead of working with infinite tiling links embedded in the non-compact manifolds $\mathbb{R}^3$ and $\mathbb{R}^2 \times I$, we quotient out by a discrete group of fixed-point free isometries to obtain a finite link in a thickened surface. Let $\widetilde{L}$ be a link derived from a Euclidean tiling and fix a fundamental domain for a $\mathbb{Z}^2$ action by translations which respect over- and under-crossings. Note that the symmetry group of every uniform tiling of the Euclidean plane contains a $\mathbb{Z}^2$ subgroup generated by translations so such a fundamental domain always exists, and the requirement that crossings be respected at most forces a doubling of the domain in each translation direction. Taking the quotient of $\mathbb{R}^3 - \widetilde{L}$ by $\mathbb{Z}^2$ yields a link L in a thickened torus $T \times (0,1)$. Note that the link complement still exists as a subspace of S^3 as we can think of $T \times (0,1)$ as the complement of the Hopf link in S^3.

The existence of a similar process for tilings derived from hyperbolic tiling links is not as immediate. To obtain the torus from $\mathbb{R}^2$ we need only find a $\mathbb{Z}^2$ subgroup in the group of isometries of our tiling, but to obtain a higher-genus surface we require a surface subgroup.

Proposition 4.1. *Any 3- or 4-regular compact tiling $\mathcal{T}$ of the hyperbolic plane can generate a link L in a thickened surface $S_g \times I$ of genus $g \geq 2$.*

Proof. Let $\mathcal{T}$ be any compact tiling of $\mathbb{H}^2$ and $G_{\mathcal{T}}$ be the group of symmetries of $\mathcal{T}$. We show $\mathcal{T}$ can be realized as a tiling of a closed surface. Note that $G_{\mathcal{T}}$ is a Coxeter group generated by reflections over the sides of the fundamental domain of $\mathcal{T}$. To find a surface group by which to quotient, we employ a result of Gordon, Long and Reid which states that a Coxeter group contains a surface group if and only if it is not virtually free ([GLR04]).

Suppose $G_{\mathcal{T}}$ is virtually free. Then there exists a free subgroup $F_n < G_{\mathcal{T}}$ of finite index. As F_n is free, its action on $\mathbb{H}^2$ defines the $\{2n, \infty\}$ paracompact tiling, and as F_n is of finite index, it has fundamental domain composed of a finite number of fundamental domains of $G_{\mathcal{T}}$. Hence a fundamental domain for $\mathcal{T}$ has an ideal vertex. But $\mathcal{T}$ was assumed to be compact. Thus $G_{\mathcal{T}}$ contains a surface subgroup $\pi_1(S_g)$ for $g \geq 2$.

Let $\widetilde{L} \subset \mathbb{R}^2 \times I$ be a tiling link derived from a tiling $\mathcal{U}$ and let $\mathcal{T}$ be the tiling defined by the symmetries of $\widetilde{L}$. Note that $G_{\mathcal{T}}$ will be a finite-index subgroup of $G_{\mathcal{U}}$. Taking a quotient by the action of a surface subgroup of $G_{\mathcal{T}}$ yields a link L in $S_g \times I$. □

Henceforth *tiling links* will refer to links living in S^3, $T \times (0,1)$ or $S_g \times I$ as defined above, rather than their infinite counterparts. For link complements in $S_g \times I$, $g > 1$, we concern ourselves exclusively with the case where $S_g \times \{0\}$ and $S_g \times \{1\}$ are totally geodesic. This satisfies the hypothesis of Theorem 2.4 to ensure that a complete hyperbolic structure of finite volume is unique if it exists. Throughout this section, we often repress the genus and refer to any thickened surface of genus $g \geq 2$ by $S \times I$.

The generalized octahedral and bipyramid decompositions apply in this context to give upper bounds on the volumes of any link complements in $S \times I$. In the octahedral upper bound, the maximal ideal octahedron with volume v_{oct} is replaced with the maximal octahedron with two opposite ideal vertices, with volume $2v_{\text{oct}}$ by Corollary 3.3. In the bipyramidal upper bound, the regular ideal bipyramids B_n^{ideal} are replaced with the maximal doubly truncated bipyramids $B_n^{\text{truncated}}$.

For links in S^3 (or $T \times (0,1)$), the bipyramid bound is best in comparison to the octahedral bound when the faces in the link projection have many edges. If most of the faces have between 4 and 10 edges, the octahedral construction gives a better bound because the tetrahedral wedges in the face-centered ideal bipyramids have larger volume than the original wedges in the crossing-centered octahedra. (This discussion does not consider drilling or collapsing, which for reasonably small knots can make the bipyramid bound much stronger, see [Ada15a].)

For links in $S \times I$, the generalized bipyramid bound is best in comparison to the generalized octahedral bound when the faces have few edges, because the tetrahedral wedges are farthest from the maximal wedge described in Corollary 3.2. As the number of edges in the faces grows, the bipyramid wedges approach the maximal wedges with volume $v_{\text{oct}}/2$ (see Figure 9b), so the bipyramid bound approaches the octahedral bound. In all cases the truncated bipyramid bound is better than the generalized octahedral bound.

4.2. **Computing volumes of tiling links.** In this section we compute the volumes for all tiling links in appropriate thickened surfaces. We use a Lagrange multiplier argument in the spirit of Lemma 3.1 and Corollary 3.4.

Theorem 4.2. *Consider a face-centered bipyramid decomposition of the complement of a tiling link. In the angle structure realizing the complete hyperbolic structure, the dihedral angles along edges incident to the apex in a given bipyramid are equal to the planar angles of the corresponding polygon in the equilateral realization of that uniform tiling.*

The statement about an equilateral realization of the tiling is irrelevant in the Euclidean case, as the angles in a uniform Euclidean tiling are independent of the side lengths. For non-Euclidean tilings, the angles may vary significantly. For instance, a spherical projection of a truncated cube with small triangular faces has very different angles than one with large triangular faces.

Proof. Let $\{\Delta_{n,1}, ..., \Delta_{n,k_n}\}$ be the collection of tetrahedra contained in n-bipyramids for a particular n, with angles as in Figure 7 with appropriate subscripts. Using Theorem 2.3, we determine the complete hyperbolic structure by finding a critical point of the volume functional subject to the various constraints. For 4-regular tilings, we use the following constraints, ranging over the indices n and i:

$$D_{n,i} + B_{n,i} + F_{n,i} = D_{n,i} + C_{n,i} + E_{n,i} = \pi$$

$$\sum_{i=1}^{k_n} A_{n,i} = 2\pi k_n$$

$$\sum_{n,i} D_{n,i} = 2\pi c(L)$$

For 3-regular tilings, the last constraint is replaced by

$$\sum_{n,i} D_{n,i} = \pi c(L),$$

because D edges at crossings on either side of a bigon region are identified.

Note that these constraints are significantly weaker than the full set of constraints required for an angle structure. In particular we consider the sum over all D angles, and all A angles for a given n, but do not explicitly require that those coming together at a single edge sum to 2π. The simplified constraints make the Lagrange multiplier method more tractable, and due to the the symmetry of the tiling the end solution will satisfy all the constraints for an angle structure.

We apply Lagrange multipliers and substitute with Schläfli's formula, as in Lemma 3.1 and Corollary 3.4. The resulting equations are, for all n, i, j:

$$\begin{aligned}\ell_{A_{n,i}} &= \ell_{A_{n,j}}\\ \ell_{D_{n,i}} &= \ell_{B_{n,i}} + \ell_{C_{n,i}} + \lambda\\ \ell_{B_{n,i}} &= \ell_{F_{n,i}}\\ \ell_{C_{n,i}} &= \ell_{E_{n,i}}\end{aligned}$$

The Lagrange multiplier λ remains unknown, but is constant across different values of n and i. Where the lengths are infinite, the equations should be understood to hold in the limit as the relevant vertices become ideal.

Now we focus on a single tetrahedron, and drop the indices for simplicity. As in the proof of Lemma 3.1, we may consider each tetrahedron in the Poincaré ball model with vertices

$$v_1 = (0, 0, 1), \quad v_2 = (0, 0, -1), \quad v_4 = (r_4, 0, 0), \quad v_3 = (r_3 \cos D \sin\phi, r_3 \sin D \sin\phi, r_3 \cos\phi).$$

Define p_B, p_C, p_E, p_F and R_B, R_E, R_F as in the proof of Lemma 3.1. By the same logic used there, the conditions $\ell_B = \ell_F$ and $\ell_C = \ell_E$ tell us that $R_B = R_E = R_F$. We claim they also imply $\phi = \pi/2$ and $r_3 = r_4$.

The vertices v_3 and v_4 are identified with the points U and D. For spherical tiling links, these vertices are finite. Thus v_4 lies on the intersection of horospheres centered at v_1 and v_2 with radii R_B, which we call H_1 and H_2. Since $R_B = R_E = R_F$, v_3 must also lie on the intersection of those horospheres in the xy-plane, so $\phi = \pi/2$ and $r_3 = r_4$. For hyperbolic tiling links v_3 and v_4 are ultra-ideal. The truncation plane for v_4 is then simultaneously tangent to H_1 and H_2. The truncation plane for v_3 must also be simultaneously tangent to H_1 and H_2, which again implies $\phi = \pi/2$ and $r_3 = r_4$ as in the proof of Lemma 3.1.

For Euclidean tiling links v_3 and v_4 are ideal, so $r_3 = r_4 = 1$, but the requirement that $\phi = \pi/2$ is not as obvious. In this case $R_B = 1$ and $H_1 = H_2$ is the boundary sphere $\partial\mathbb{H}^3$. Instead we consider horospheres H_1' and H_2' centered at v_1 and v_2 with Euclidean radii $\frac{1}{2}$, tangent to each other at the origin. Let H_4 be a horosphere centered at v_4 and tangent to H_1', by symmetry also tangent to H_2'. Let H_{3E} and H_{3F} be horospheres centered at v_3, tangent to H_1' and H_2' respectively. Consider the hyperbolic radii of these spheres as all the vertices limit to ideal points. Throughout the limiting process we require the spheres to maintain the points of tangency specified. Let ρ_i denote the hyperbolic radius of sphere H_i, with primes as necessary. The conditions $\ell_B = \ell_F$ and $\ell_C = \ell_E$ then become

$$\begin{aligned}\lim(\rho_1' + \rho_4) &= \lim(\rho_1' + \rho_{3F}),\\ \lim(\rho_1' + \rho_4) &= \lim(\rho_1' + \rho_{3E}),\end{aligned}$$

where the limits are taken as the vertices become ideal. These equations then imply

$$\lim(\rho_{3F} - \rho_{3E}) = 0.$$

That difference can be evaluated in the limit as the finite distance between the concentric horospheres H_{3E} and H_{3F}. We conclude that $H_{3E} = H_{3F}$, thus $\phi = \pi/2$ by symmetry.

We have established that

$$v_3 = (r_3 \cos D, r_3 \sin D, 0).$$

Symmetry now shows

$$B_{n,i} = C_{n,i} = E_{n,i} = F_{n,i} = \frac{\pi - D_{n,i}}{2}.$$

By explicit computation the angle A between the top and bottom faces of the tetrahedron is

$$A = \arccos(-1 + r_4^2 + r_4^2 \cos D).$$

Solving for r_4,

$$r_4 = \sqrt{\frac{1 + \cos A}{1 + \cos D}}.$$

Now we show that every tetrahedron in the decomposition, when isometrically placed in the Poincaré ball model as described above, must have the same value of r_4. From the Lagrange multiplier equation

$$\ell_{D_{n,i}} - \ell_{B_{n,i}} - \ell_{C_{n,i}} = \lambda$$

we know that λ is twice the distance between the horospheres H_1 and H_1'. In particular, fixing the value of λ fixes the value of R_B. When v_4 is finite,

$$R_C = \frac{1}{2}(r_4^2 + 1),$$

and when it is ultra-ideal

$$R_C = \frac{1}{1 + \sqrt{r_4^2 - 1}}.$$

Each of these functions is one-to-one, so for fixed R_B there are at most two possibilities for r_4. When there are two possibilities, one corresponds to finite apexes for the bipyramid and the other corresponds to ultra-ideal apexes. Since all the bipyramids share the same apexes, they must all have the same value r_4. Once r_4 is fixed, ℓ_A increases monotonically with the angle D so the condition $\ell_{A_{n,i}} = \ell_{A_{n,j}}$ forces $D_{n,i} = D_{n,j}$ and $A_{n,i} = A_{n,j} = 2\pi/n$. With this, all the conditions for an angle structure are satisfied.

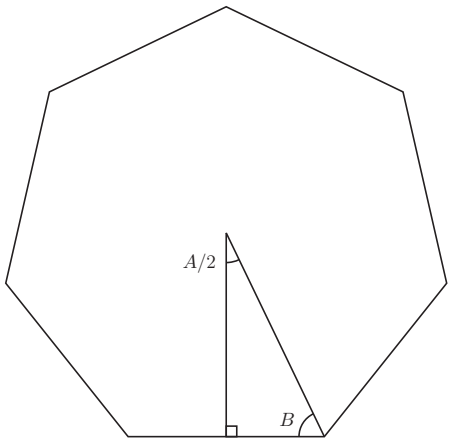

FIGURE 12. A right triangle as in the proof of Theorem 4.2.

Finally, we show that the bipyramid angles $2B_{n,i}$ are the internal angles of n-gons in the equilateral realization of this tiling. Consider a regular n-gon with interior angles $2B = \pi - D$ and side lengths L. Draw a right triangle by connecting the center of the polygon to one vertex and to the midpoint of an adjacent side (see Figure 12). The right triangle has angles $A/2$ and B. If it is a spherical triangle, then spherical trigonometry tells us

$$\cos\frac{L}{2} = \frac{\cos(\frac{A}{2})}{\sin B} = \sqrt{\frac{1+\cos A}{1-\cos 2B}} = r_4.$$

Similarly if it is a hyperbolic triangle, then hyperbolic trigonometry tells us

$$\cosh\frac{L}{2} = r_4.$$

The condition that r_4 must be the same for every tetrahedral wedge thus tells us that the dihedral angles $2B$ of the bipyramids are the internal angles of the corresponding hyperbolic polygons in an equilateral realization of that tiling. □

Theorem 4.2 allows us to easily compute the volumes of all tiling links. For spherical tilings these volumes have additional significance. When L is alternating, the projection graph of L gives a net for each polyhedron. In [Men83], Menasco gives a decomposition of $S^3 - L$ into two isometric polyhedra. By splitting the bipyramidal decomposition of a spherical tiling link into top and bottom pyramids and gluing the tops and bottoms around the vertex links of U and D, respectively, we recover Menasco's decomposition. Thus

for an alternating link L derived from a spherical tiling we obtain a decomposition of $S^3 - L$ into two copies of the polyhedron associated to the spherical tiling.

Corollary 4.3. *A link $L \subset S^3$ corresponding to a spherical tiling has volume exactly twice that of the maximal hyperbolic polyhedron of the same combinatorial description.*

The volumes of these polyhedra are enumerated in Figure 13 along with the angles of their associated spherical tilings. It is interesting to note that numerical evidence shows that for a spherical tiling link, the complete hyperbolic structure occurs at a complex critical point of the volume functional, not a simple maximum.

Solid	Vertex configuration	Angles	vol(L)/2
tetrahedron	3.3.3	$\frac{2\pi}{3}.\frac{2\pi}{3}.\frac{2\pi}{3}$	$v_{\text{tet}} \approx 1.0149$
octahedron	3.3.3.3	$\frac{\pi}{2}.\frac{\pi}{2}.\frac{\pi}{2}.\frac{\pi}{2}$	$v_{\text{oct}} \approx 3.6639$
cube	4.4.4	$\frac{2\pi}{3}.\frac{2\pi}{3}.\frac{2\pi}{3}$	5.0747
dodecahedron	5.5.5	$\frac{2\pi}{3}.\frac{2\pi}{3}.\frac{2\pi}{3}$	20.5802
truncated tetrahedron	3.6.6	(1.17).(2.56).(2.56)	8.2957
cuboctahedron	3.4.3.4	(1.23).(1.91).(1.23).(1.91)	12.0461
truncated cube	3.8.8	(1.10).(2.59).(2.59)	20.8916
truncated octahedron	4.6.6	(1.68).(2.30).(2.30)	25.2238
rhombicuboctahedron	3.4.4.4	(1.13).(1.72).(1.72).(1.72)	31.6987
truncated cuboctahedron	4.6.8	(1.62).(2.18).(2.48)	57.2688
icosidodecahedron	3.5.3.5	(1.11).(2.03).(1.11).(2.03)	39.8793
truncated dodecahedron	3.10.10	(1.06).(2.61).(2.61)	61.5356
truncated icosahedron	5.6.6	(1.94).(2.17).(2.17)	77.7139
rhombicosadodecahedron	3.4.5.4	(1.08).(1.62).(1.96).(1.62)	92.7191
truncated icosidodecahedron	4.6.10	(1.59).(2.13).(2.57)	155.4566

FIGURE 13. Volumes of maximal ideal Archimedean solids.

In Figure 14 we give explicit values for the volume densities $\mathcal{D}(L)$ of links in appropriate thickened surfaces.

4.3. **Volume density in $S \times I$.** In addition to finding exact values for the volumes of links in $T \times (0,1)$ and $S \times I$, we can also ask about the set of their volume densities vol(L)/$c(L)$. The generalized octahedral construction with U and D ideal immediately gives the following lemma.

Lemma 4.4. *The volume density of a link L in a thickened torus $T \times (0,1)$ is at most v_{oct}.*

Note that this result also follows from the fact that a hyperbolic link in $T \times I$ can be thought of as a link in the complement of the Hopf link, and therefore corresponds to a link in S^3. As previously mentioned, hyperbolic links in S^3 have an upper bound of v_{oct} on their volume densities.

The generalized bipyramid construction with U and D ultra-ideal, along with Corollaries 3.2 and 3.4 immediately gives the equivalent result for $S \times I$.

Lemma 4.5. *The volume density of a link L in a thickened surface $S \times I$ is strictly less than $2v_{oct}$.*

Lemma 4.6. *There exists a sequence of links L_n in thickened surfaces $S_n \times I$ with volume densities approaching $2v_{oct}$.*

Tiling link	$\mathcal{D}(L)$
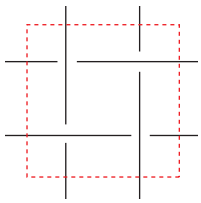 4.4.4.4	$v_{\text{oct}} \approx 3.6639$
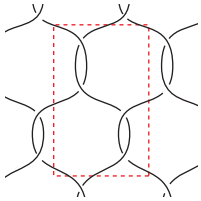 6.6.6	3.0448
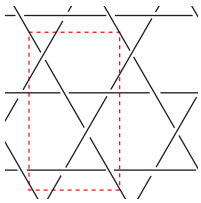 3.6.3.6	3.3831
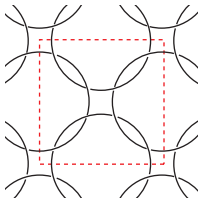 4.8.8	2.8797
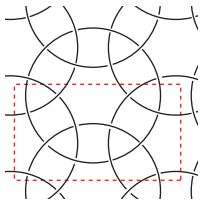 3.4.6.4	3.5235

(A) Volume densities for Euclidean tiling links.

Tiling link	Minimal genus	$\mathcal{D}(L)$
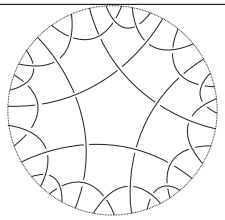 5.5.5.5	2	5.4535
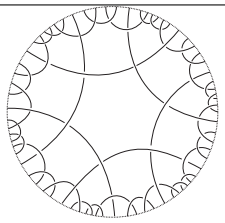 6.6.6.6	2	6.1064
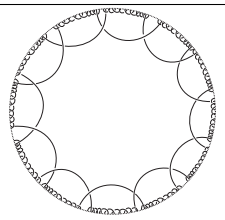 12.12.12.12	2	7.0470
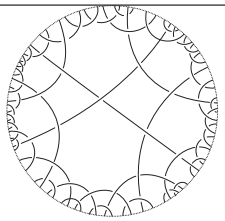 4.8.4.8	2	5.4581
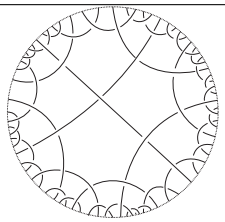 5.6.5.6	3	5.7962

(B) Volume densities for hyperbolic tiling links.

FIGURE 14. Volume densities for links in thickened surfaces.

Proof. For $n > 1$, let $\widetilde{L_n}$ be an infinite tiling link derived from the $\{n, 4\}$ tiling of $\mathbb{H}^2$ and S_n be a closed surface such that its fundamental group is a subgroup of the Coxeter group of symmetries of $\widetilde{L_n}$. Suppose a fundamental domain for S_n is composed of k n-gons, and let L_n denote the tiling link in $S_n \times I$ after quotienting by the appropriate surface group. Note that there will be k n-gons in a projection of L_n onto

$S_n \times \{0\}$. By Theorem 4.2 the volume of $(S_n \times I) - L_n$ is $k\text{vol}(B_n^{\square})$ where $B_n^{\square}$ denotes the generalized n-bipyramid with all dihedral angles equal to $\pi/2$. The crossing number of the resulting link L_n in $S_n \times I$ is seen to be $nk/4$ by results in [AFLT02]. Hence the volume density of L_n in $S_n \times I$ is $4\text{vol}(B_n^{\square})/n$ and as in the discussion following Corollary 3.4,

$$\lim_{n\to\infty} \frac{4\text{vol}(B_n^{\square})}{n} = 2v_{\text{oct}}.$$

□

Theorem 4.7. *The set of volume densities of links in $S_g \times I$ across all genera $g \geq 2$, assuming totally geodesic boundary, is a dense subset of the interval $[0, 2v_{oct}]$.*

Proof. Let $x \in (0, 2v_{\text{oct}})$ and $\epsilon > 0$. By Lemma 4.6, there exists a link L in a thickened surface $S \times I$ such that $\mathcal{D}(L) = \text{vol}(L)/c(L) > x$. Thus $x = \text{vol}(L)/(c(L) + d)$ for some real $d > 0$. By taking an n-fold cyclic cover of $(S \times I) - L$ around one handle we may scale the volume and crossing number by n. Drilling out an unknotted augmenting component around any crossing of the resulting link preserves hyperbolicity and raises the volume by some amount $b_n > 0$ which may depend on n and the particular choice of drilling [Ada15b]. Then we perform $(1, t_n)$-Dehn filling on the augmenting component, replacing the crossing with a twist region of $t_n + 1$ crossings to create a link L' with volume bounded above by $n\text{vol}(L) + b_n$ and crossing number $nc(L) + t_n$. Set

$$t_n = \left\lfloor \frac{n\text{vol}(L) + b_n}{x} \right\rfloor - nc(L).$$

Then, for sufficiently large n, $t_n > 2\pi$ so L' is hyperbolic and moreover,

$$\mathcal{D}(L') \leq \frac{n\text{vol}(L) + b_n}{nc(L) + t_n} = x + \frac{n\text{vol}(L) + b_n - x\left\lfloor \frac{n\text{vol}(L)+b_n}{x} \right\rfloor}{\left\lfloor \frac{n\text{vol}(L)+b_n}{x} \right\rfloor} < x + \frac{x}{\left\lfloor \frac{n\text{vol}(L)+b_n}{x} \right\rfloor} < x + \epsilon.$$

Note that by our choice of t_n,

$$t_n > \left\lfloor \frac{n\text{vol}(L)}{x} \right\rfloor - nc(L) > nd - 1$$

and also

$$\frac{n\text{vol}(L) + b_n}{nc(L) + t_n} \geq x.$$

A result of Futer, Kalfagianni, and Purcell [FKP08] provides a bound for the amount the volume can drop due to Dehn filling along a slope s,

$$\text{vol}(L') \geq \left(1 - \left(\frac{2\pi}{\ell}\right)^2\right)^{3/2} (n\text{vol}(L) + b_n),$$

where ℓ is the length of s. Since t_n (and thus ℓ) increases without bound as n does, we can choose n sufficiently large such that

$$\left(1 - \left(\frac{2\pi}{\ell}\right)^2\right)^{3/2} > \frac{x}{x+\epsilon},$$

so then

$$\mathcal{D}(L') \geq \left(1 - \left(\frac{2\pi}{\ell}\right)^2\right)^{3/2} \frac{n\text{vol}(L) + b_n}{nc(L) + t_n} > \frac{x^2}{x+\epsilon} > x - \epsilon.$$

□

Note that cyclic covers of tori remain tori and hence the following result can be deduced through arguments similar to those above.

Corollary 4.8. *The set of volume densities for links in $T \times (0, 1)$ is a dense subset of the interval $[0, v_{oct}]$.*

Taking cyclic covers of a surface of genus $g \geq 2$ increases the number of handles, prompting us to consider the set of volume densities in surfaces of a fixed genus. As mentioned in the introduction, we define the genus for non-orientable surfaces in terms of the Euler characteristic χ as $g = (2 - \chi)/2$, so that "fixed genus" directly translates to "fixed Euler characteristic".

Proposition 4.9. *The maximum volume density for links in thickened surfaces of fixed genus $g \geq 2$ is given by*

$$\beta_g := \frac{\mathrm{vol}(B^{\square}_{8g-4})}{2g-1}$$

and is realized by a tiling link derived from the $\{8g-4, 4\}$ tiling in a closed non-orientable surface of genus g.

Proof. The complement of a link L in $S_g \times I$ decomposes into $c(L)$ generalized octahedra, which then break up into $4c(L)$ tetrahedra Δ_i with two ideal vertices each. Label the dihedral angles of Δ_i as in Figure 7. The ideal vertices and edge gluings around the core lines of the octahedra impose the constraints

$$D_i + B_i + F_i = D_i + C_i + E_i = \pi,$$

$$\sum_{i=1}^{4c(L)} D_i = 2\pi c(L).$$

Additionally, the truncation triangles of the tetrahedra must tile $S_g \times \{0\}$ and $S_g \times \{1\}$, so by Gauss-Bonnet we have

$$\sum_{i=1}^{4c(L)} (\pi - A_i - B_i - C_i) = \sum_{i=1}^{4c(L)} (\pi - A_i - E_i - F_i) = -2\pi(2-2g).$$

Combining with the previous constraints yields

$$\sum_{i=1}^{4c(L)} A_i = 2\pi(2 - 2g + c(L)).$$

Now we have effectively the same system of constraints as in Theorem 4.2, so as then they imply $B_i = C_i = E_i = F_i = (\pi - D_i)/2$, $D_i = D_j$, and $A_i = A_j$ for all i and j. Plugging back in to the constraints, we get $D_i = \pi/2$, $B_i = C_i = E_i = F_i = \pi/4$.

The volume density is simply the combined volume of four of these tetrahedra, which are as large as possible when A_i is as small as possible, which is to say when $c(L)$ is as small as possible. By Euler characteristic considerations, the minimum number of crossings comes from a tiling by a single $(8n-4)$-gon. The edge identifications on a single polygon which respect over- and under-crossings produce a non-orientable surface. □

We conclude with a few open questions.

Question 1. *Is the set of volume densities of links in $S_g \times I$ for fixed genus $g \geq 2$ dense in $[0, \beta_g]$?*

Augmentation and taking a belted sum with links in S^3 leaves genus intact, and thus the set of volume densities of links in $S_g \times I$ can be shown to be dense in $[0, v_{oct}]$ by employing results of, e.g., [Bur15] and [ACJ+15].

Question 2. *Can bipyramidal decompositions be used to compute the volume of non-alternating tiling links?*

Question 3. *Can bipyramidal decompositions be used to compute the volumes of links derived from non-uniform tilings?*

In both of the preceding questions, the bipyramids are unlikely to remain regular, and some skewing factor should be taken into account to determine the complete hyperboliic structure and calculate exact volumes.

References

[ACJ+15] Colin Adams, Aaron Calderon, Xinyi Jiang, Alexander Kastner, Gregory Kehne, Nathaniel Mayer, and Mia Smith, *Volume and determinant densities of hyperbolic rational links*, Arxiv 1510.06050 (2015), 1–8.

[Ada15a] Colin Adams, *Bipyramids and bounds on volumes of hyperbolic links*, Arxiv 1511.02372 (2015), 1–13.

[Ada15b] ———, *Generalized augmented alternating links and their volumes*, ArXiv 1506.03026 (2015), 1–17.

[AFLT02] Colin Adams, Thomas Fleming, Michael Levin, and Ari M. Turner, *Crossing number of alternating knots in sxl*, Pacific J. Math. **203** (2002), 1–22.

[Bra17] H. R. Brahana, *A proof of petersen's theorem*, Annals of Mathematics **19** (1917), no. 1, pp. 59–63 (English).

[Bur15] S. D. Burton, *The Spectra of Volume and Determinant Densities of Links*, ArXiv 1507.01954 (2015), 1–18.

[CKP15a] A. Champanerkar, I. Kofman, and J. Purcell, *Geometrically and diagrammatically maximal knots*, ArXiv 1411.7915 (2015), 1–25.

[CKP15b] A. Champanerkar, I. Kofman, and J. S. Purcell, *Volume bounds for weaving knots*, ArXiv 1506.04139 (2015), 1–14.

[FG11] David Futer and François Guéritaud, *From angled triangulations to hyperbolic structures*, Interactions between hyperbolic geometry, quantum topology and number theory, Contemp. Math., Amer. Math. Soc. **541** (2011), 159–182.

[FKP08] David Futer, Efstratia Kalfagianni, and Jessica S Purcell, *Dehn filling, volume and the jones polynomial*, Journal of Differential Geometry (2008), no. 78, 429–464.

[FP04] Roberto Frigerio and Carlo Petronio, *Construction and recognition of hyperbolic 3-manifolds with geodesic boundary*, Trans. Amer. Math. Soc. **356** (2004), no. 8, 3243–3282 (electronic).

[GLR04] C. McA Gordon, D. D. Long, and a. W. Reid, *Surface subgroups of Coxeter and Artin groups*, Journal of Pure and Applied Algebra **189** (2004), no. 1-3, 135–148.

[Kel89] Ruth Kellerhals, *On the volume of hyperbolic polyhedra*, Mathematische Annalen **285** (1989), no. 4, 541–569.

[LST08] Feng Luo, Saul Schleimer, and Stephan Tillmann, *Geodesic ideal triangulations exist virtually*, Proc. Amer. Math. Soc. **136** (2008), 2625–2630.

[LY14] Feng Luo and Tian Yang, *Volumes and rigidity of hyperbolic polyhedral 3-manifolds*, ArXiv 1404.5365 (2014), 129.

[Men83] W. Menasco, *Polyhedra representation of link complements*, Low-dimensional topology (San Francisco, Calif., 1981), Contemp. Math., vol. 20, Amer. Math. Soc., Providence, RI, 1983, pp. 305–325.

[Pet91] Julius Petersen, *Die theorie der regulären graphs*, Acta Mathematica **15** (1891), no. 1, 193–220.

[Riv94] Igor Rivin, *Euclidean structures on simplicial surfaces and hyperbolic volume*, Annals of Mathematics **139** (1994), no. 3, pp. 553–580.

[Sch50] Ludwig Schläfli, *Theorie der vielfachen kontinuität*, Gesammelte Mathematische Abhandlungen, Springer Basel, 1950, pp. 167–387.

[Ush06] Akira Ushijima, *A volume formula for generalized hyperbolic tetrahedra*, Non-Euclidean geometries, Math. Appl. (N. Y.), Springer, New York **581** (2006), 249265.

(Colin Adams) Williams College
E-mail address: colin.c.adams@williams.edu

(Aaron Calderon) University of Nebraska-Lincoln
E-mail address: aaron.calderon@huskers.unl.edu

(XinYi Jiang) Stanford University
E-mail address: xinyij@stanford.edu

(Alexander Kastner) Williams College
E-mail address: ask2@williams.edu

(Gregory Kehne) Williams College
E-mail address: gtk1@williams.edu

(Nathaniel Mayer) Harvard University
E-mail address: nmayer26@gmail.com

(Mia Smith) Williams College
E-mail address: mia.smith25@gmail.com